Journal of Catalysis **195,** 304–315 (2000)
doi:10.1006/jcat.2000.2989, available online at http://www.idealibrary.com on IDEAL®

Characterization of Pd–Au/SiO_2 Catalysts by X-ray Diffraction, Temperature-Programmed Hydride Decomposition, and Catalytic Probes

M. Bonarowska, J. Pielaszek, W. Juszczyk, and Z. Karpiński[1]

Institute of Physical Chemistry, Polish Academy of Sciences, ul. Kasprzaka 44/52, PL 01-224 Warszawa, Poland

Received February 28, 2000; revised May 23, 2000; accepted July 14, 2000

Two series of Pd–Au/SiO_2 catalysts, differing widely in metal particle size distribution, were prepared by a direct redox method, which involves reductive deposition of gold onto prereduced palladium particles. The method yields good results; i.e., a significant Pd–Au alloying was achieved in reduced bimetallic catalysts. The catalysts were investigated at various stages of their preparation by X-ray diffraction and temperature-programmed hydride decomposition. These techniques appear valuable in assessing the degree of alloying. Being sensitive to palladium particle size, the temperature-programmed hydride decomposition could also be applied to estimate the palladium dispersion. 2,2-Dimethylpropane conversion carried out on Pd–Au/SiO_2 also appeared to be a useful probe. Apparent activation energy decreased considerably with gold addition. This result is contrary to a relative constancy of the activation energy observed earlier for Pd–Au/SiO_2 catalysts, which were prepared by an incipient wetness coimpregnation when the resulting bimetallic samples were not satisfactorily homogenized.

Key Words: **Pd–Au/SiO_2; probing degree of homogeneity; X-ray diffraction; temperature-programmed hydride decomposition (TPHD); 2,2-dimethylpropane conversion.**

1. INTRODUCTION

Supported Pd–Au bimetallic catalysts play an important role in chemical technology (1). They are commonly used in catalytic hydrogenation of organic compounds (1, 2) and production of vinyl acetate (3). Although gold is essentially inactive in a majority of applicable catalytic processes, its addition to palladium often enhances overall activity, product selectivity, and catalyst's stability. For instance, it is claimed that addition of gold significantly improves the catalytic performance of palladium in chlorofluorocarbons (CFCs) hydrodechlorination (4, 5). In this respect, we have recently found that introduction of Au to Pd/MgF_2 notably increases the selectivity toward CH_2F_2, a desired product in CCl_2F_2 (CFC-12) hydrodechlorination (6). Since a similar amount of Au doping does not modify the catalytic behaviour of a Pd/C catalyst (7), it has been concluded that adequate Pd–Au bimetal homogeneity is essential for achieving the catalytic improvement. X-ray diffraction and temperature-programmed studies confirmed that substantial Pd–Au interactions were obtained in the case of the Pd–Au/MgF_2, but not for Pd–Au/C (7).

The preparation leading to the formation of a well-homogenized bimetallic system and its characterization, especially in the case of highly dispersed, low-loaded bimetal/supported catalysts, still present very real difficulties (8). Preparation of supported Pd–Au alloys has been a subject of numerous studies for many years (the period until 1972 is covered in Ref. (9)). Several preparation procedures either resulted in insufficient alloy homogeneity (10, 11) or showed the necessity of using very high temperature pretreatment for obtaining proper alloying, e.g., 900°C in a vacuum (11, 12). Such a preparation would lead either to an undesirable metal sintering or to strong metal–support interactions. Among a few successful, well-documented, Pd–Au/support preparations, one should mention the work by Lam and Boudart (13), where very small Pd–Au particles (2.0–4.5 nm in size) were prepared by ion exchange of $[Au(en)_2]^{3+}$ and $[Pd(NH_3)_4]^{2+}$ with silica and reduction at temperatures up to 300°C. More recent EXAFS studies of such catalysts confirmed the formation of Pd–Au bimetallic clusters (14).

In our present search for the preparation of well-mixed supported Pd–Au catalysts, it appeared interesting to use the direct redox method developed by Barbier and his colleagues (for review, see Ref. (15)). The method is based on the fact that due to a difference in standard electrochemical potentials a noble metal is depositing over a less-noble one. In such a preparation process, more readily reducible gold ions should be directly reduced by prereduced palladium species (Pd^0), resulting in an intimate contact of both metals.

Structural characterization of highly dispersed bimetallic catalysts is also not an easy task. Generally, *in situ* high-resolution analytical electron microscopy and EXAFS

[1] To whom correspondence should be addressed. E-mail: zk@ichf.edu.pl.

0021-9517/00 $35.00

appear to be the most suitable techniques for probing the structure and composition of supported bimetallic particles. For a routine analysis of a series of bimetallic catalysts one should search for other, preferably more common, techniques. In the case of palladium-based systems this seems to be possible. When a precursor of a palladium catalyst is reducible at low temperature, the trace of a temperature-programmed reduction run often exhibits a characteristic, relatively sharp, negative peak with a minimum at ∼100°C, what is associated with the decomposition of a β-hydride phase (16, 17). An absence of such a peak is considered as a token of palladium-phase modification, caused either by mixing with another metal (e.g., Pd–Cu/SiO_2 (18), Pd–Fe/NaY (19), Pd–Tl/Al_2O_3 (20), and Pd–Re/Al_2O_3 (21)) or palladium–support interactions (Pd-SiO_2 (22) and Pd–TiO_2 (16)). In our characterization of the prepared Pd–Au/SiO_2 catalysts, an attempt has been undertaken to exploit variations in the stability of a β-hydride phase caused by gold dissolution in palladium (23). Obviously, such a probing would give suitable results only for samples that form a hydride phase, typically in the range 50–100 at.% Pd. If a gradual introduction of Au to Pd/SiO_2 progressively leads to a decrease of hydrogen solubility in a Pd-containing phase (changes in H/Pd), then a substantial degree of alloying is manifested. More than 30 years ago, when temperature-programmed techniques were not widely used, Joice *et al.* (24) observed Pd–H and Pd–Au–H decomposition by manually raising the temperature. Their study with pumice-supported catalysts showed not only a different amount of evolved hydrogen (H/Pd vs Au content) but also a decreased stability of the PdAuH (compared to Pd–H) phase demonstrated as a downward shift of the decomposition temperature. To the best of our knowledge, a more detailed study of temperature-programmed hydride decomposition (TPHD) of supported Pd–Au catalysts has not been reported. Probing supported Pd-based catalysts with TPHD is complicated by the fact that the composition (H/Pd) and stability of the β-hydride phase are also a function of palladium particle size (25). Therefore, it is essential to have appropriate control over the dispersion of a supported palladium-containing phase when the effect of alloying is investigated.

In this work, the Pd–Au/SiO_2 catalysts prepared by a direct redox reaction were characterized by TPHD, XRD, and 2,2-dimethylpropane conversion.

2. EXPERIMENTAL

2.1. Catalyst Preparations and Pretreatments

The support was Davison 62 silica gel, 75–120 mesh, washed with diluted HCl and redistilled water, dried in the oven at 120°C for 21 h, and finally, calcined in air in an oven at 450°C for 4 h.

Two Pd/SiO_2 catalysts were prepared: 1.1 wt% Pd/SiO_2 catalyst, designated Pd(A), was prepared by ion exchange using $Pd(NH_3)_4(NO_3)_2$ (Alfa Produkte, Karlsruhe, Germany), between pH 9.6 and 10, and at room temperature (RT). The suspension obtained was filtered and carefully washed with aqueous NH_3. The solid was dried in air in an air oven at 60°C for 8 h, transferred to a glass-stoppered bottle, and kept in a desiccator.

Then, a 2 wt% Pd/SiO_2 catalyst, designated Pd(B), was prepared by impregnation of silica with an aqueous solution of palladium dichloride, using an incipient wetness technique. After impregnation, the solid was dried in an air oven at 120°C for 8 h. After drying, the material was precalcined in a fluidized bed in an air flow from RT to 450°C at a 3°/min ramp and maintained at 450°C for 3 h. After cooling down, the precursor was flushed out with Ar and reduced in a 50% H_2/Ar stream from RT to 390°C (a 3°/min ramp) and kept at 390°C for 1 h. After reduction, the catalyst was cooled down to RT in an Ar flow, passivated by a few portions of injected air, transferred to a glass-stoppered bottle, and kept in a desiccator.

Visual inspection by means of a magnifying glass revealed that the Pd(A) catalyst was rather homogeneous (greyish color) whereas the Pd(B) appeared to be composed from two fractions: a greyish material similar to that shown by the Pd(A) sample in the company of bigger, very dark, practically black grains. XRD examination established that the last catalyst was composed of very large Pd crystallites (∼100 nm in size) and some part of an almost amorphous material, as judged from an overlapping very sharp (111) diffraction peak and a very diffuse, nearly featureless (111) Pd reflection (Fig. 1). In the case of Pd(A) only a featureless background profile was observed. It became clear that these two catalysts differed very much in distribution of palladium over SiO_2 and this fact allowed us to test how the redox method of gold deposition worked in the case of so very different palladium materials.

The Pd/SiO_2 catalysts described above were modified by introducing gold in the reaction system similar to that used by Barbier *et al.* (26). A monometallic catalyst was prereduced in the reactor, purged in an argon flow, and then immersed in redistilled water. The solution was continuously stirred by bubbling argon. Then, an aqueous solution of ammonium chloroaurate (specpure from Johnson Matthey, England) was slowly introduced into the reactor. The solution was stirred with bubbling argon for the next 20 min. Finally, the resulted solid was separated by filtration, washed with redistilled water, and dried in flowing argon at 60–65°C for 11 h. The palladium and gold concentrations of the catalysts were determined using atomic absorption spectroscopy. Table 1 presents the basic characteristics of all Pd–(Au)/SiO_2 (series A and B) catalysts studied in this work.

Several experiments were also performed with Pd powder, 99.95% pure, fraction 0.25–0.55 μm (Alfa Ventron).

TABLE 1

Characteristics of Silica-Supported Palladium and Pd–Au Catalysts after Preparation

Catalyst[a]	Metal content, wt% palladium	gold	Preliminary visual and XRD inspection
			Series A
Pd(A)	1.1	—	uniform greyish; v. diffuse XRD peaks[b]
$Pd_{0.90}Au_{0.10}$	1.1	0.23	as above
$Pd_{0.80}Au_{0.20}$	1.0	0.46	uniform; two diffuse XRD peaks (highly dispersed Pd-rich and Au-rich phases[c])
			Series B
Pd(B)	2.0	—	not uniform (black grains + greyish material); bimodal distribution of Pd[b]
$Pd_{0.95}Au_{0.05}$	2.0	0.19	not uniform; XRD: sharp Pd peak overlapping diffuse reflections from Pd and 37 at.% Au phase
$Pd_{0.80}Au_{0.20}$	1.5	0.69	not uniform; XRD: sharp Pd peak overlapping diffuse reflections from almost pure Pd and almost pure Au; some presence of 30–35 at.% Au phase[d]
$Pd_{0.60}Au_{0.40}$	1.2	1.5	as above

[a] In catalyst designation, subscripts denote atomic fractions of Pd and Au in metal phase.
[b] XRD profile shown in Fig. 3.
[c] XRD profile shown in Fig. 2.
[d] XRD profile shown in Fig. 4.

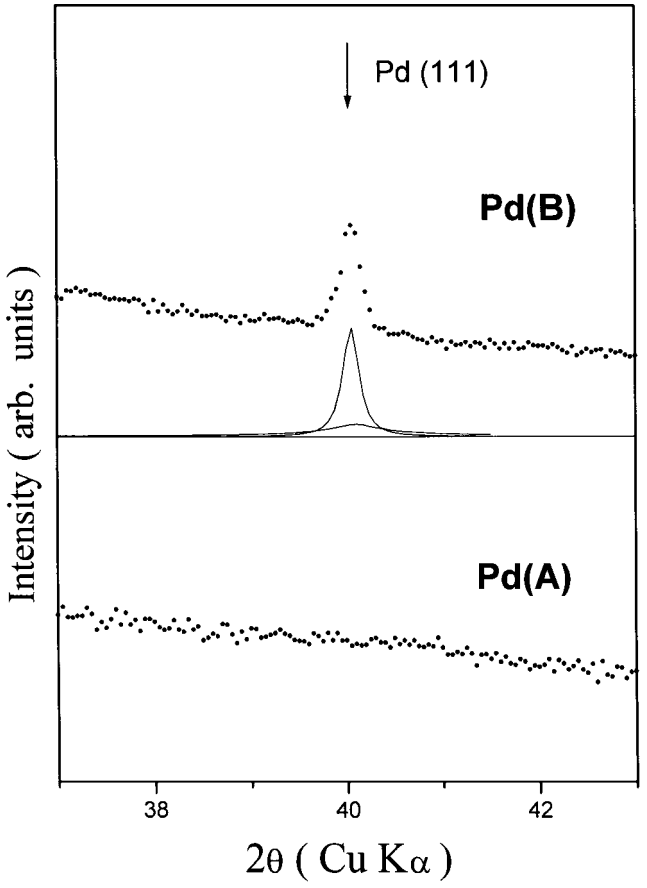

FIG. 1. XRD of 1.1 wt% Pd/SiO_2 (denoted as Pd(A)) and 2 wt% Pd/SiO_2 (denoted as Pd(B)). For Pd(B), the bottom section shows profile decomposition into Pearson VII-type functions.

2.2. Catalyst Characterization

Temperature-programmed experiments were performed in a standard apparatus equipped with a Gow-Mac thermal conductivity detector and data acquisition by a microcomputer. After preparation, the catalysts (~0.25 g) were studied by temperature-programmed reduction (TPR). In such experiments, the temperature was ramped from RT to 400°C at 8°C/min, in a flow of 10% H_2/Ar (25 cm^3 min^{-1}, purified by passing over MnO/SiO_2). After the TPR profile was collected, the sample was kept in H_2/Ar flow at 400°C for 1 or 3 h.

After TPR runs and reduction at 400°C for 1 h (or 3 h), the samples were purged with Ar for 1 h at 400°C, cooled down to 70°C, and subjected to metal dispersion measurements by hydrogen pulse chemisorption. Since it is widely accepted that hydrogen chemisorption is a good method for measuring palladium dispersion, we shall denote palladium dispersion by FE (fraction exposed). In the case of Pd–Au samples, when hydrogen uptake (per Pd atom) would be suppressed (due to the presence of gold), we shall refer to those data as D_h. After chemisorption, the samples were cooled down to ~0°C and subjected to subsequent temperature-programmed study in 10% H_2/Ar flow, ramping the temperature from ~0 to 150°C, at 7°C/min. Since the samples had already been reduced, the aim of such experiments was to monitor hydrogen evolution in the process of β-hydride decomposition. Accordingly, such testing is termed temperature-programmed hydride decomposition (TPHD).

XRD measurements were performed on a standard Rigaku-Denki diffractometer using Bragg-Brentano

focusing geometry and Ni-filtered Cu $K\alpha$ radiation. After preparation and various pretreatments, the catalysts were scanned by a step-by-step technique. The obtained XRD profiles were fitted to an analytical function of the PEARSON-VII type using commercial PEAKFIT software (Peakfit, Version 3.11, Jandel Scientific GmbH, D-40699 Erkharth, Germany). For phase identification and calculation of the phase composition, centroids of the fitted profiles were used, and for the calculation of the crystallite size, the half-widths of the fitted profiles were taken.

2.3. Catalytic Conversion of 2,2-Dimethylpropane

The reaction of 2,2-dimethylpropane (22DMP, Merck) in excess hydrogen (purified over MnO/SiO_2) was conducted in a glass flow reactor system under atmospheric pressure. 22DMP was purified by passing it through a 5A molecular sieve trap to remove any *n*-butane impurity from the reactant stream. Feed partial pressures were 22DMP, 6 Torr (1 Torr = 133.3 N m^{-2}), and hydrogen, 60 Torr. Helium was a diluent gas. Total flow was 75 cm^3 min^{-1}. The reaction was followed by gas chromatography (HP5890 with FID, 6-m squalane/Chromosorb P column). To avoid secondary reactions and limit self-poisoning, overall conversions were usually kept low, i.e., below 1%. After reduction, the catalyst (0.1–0.3 g, depending on metal loading and dispersion, and Pd/Au ratio) was brought into contact with the reaction mixture at a relatively low reaction temperature (230°C, typically). If the conversion level was found well below 1%, the temperature was increased in small increments, up to obtaining ~1% conversion. At this stage, the temperature was stabilized and the time-on-stream behavior was studied (Fig. 2). After stable conversion at the highest reaction temperature was reached (after ~1.5 h), the reaction temperature was gradually decreased at ~10°C intervals and next experimental values were collected (at least two for each temperature). Turnover frequencies (TOFs) were calculated on the basis of metal dispersion values, H/Pd, known from hydrogen chemisorption. Initial product distributions (=selectivities) were calculated as the carbon percentage of a hydrocarbon consumed in the formation of a designated product. For instance, the mol% of methane from 2,2-dimethylpropane would be divided by 5 and normalized in deriving the product distribution.

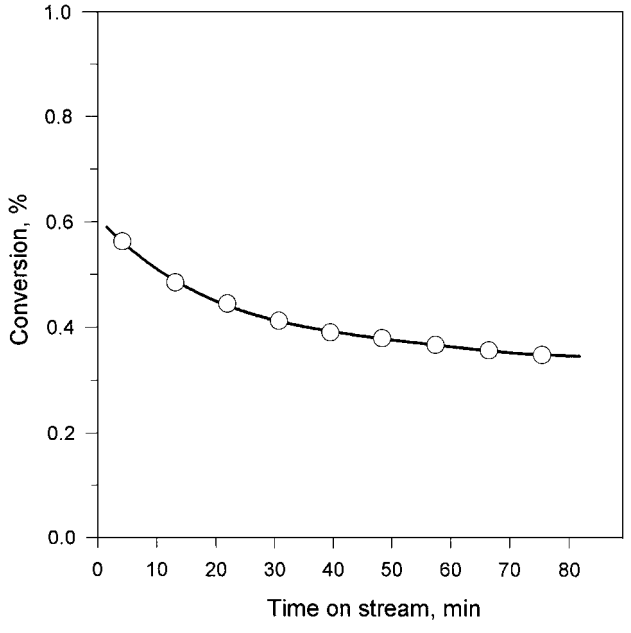

FIG. 2. Time-on-stream behavior of $Pd_{0.60}Au_{0.40}/SiO_2$ (series B) in 2,2-dimethylpropane conversion. Reaction temperature, 323°C; mass of catalyst, 0.297 g.

3. RESULTS AND DISCUSSION

In our previous work (10) when using an incipient wetness technique for coimpregnation of silica with a chloride solution of both metals, we did not succeed in preparing properly mixed Pd–Au/SiO_2 catalysts. Interest in preparation of well-alloyed Pd–Au catalysts for use in CCl_2F_2 (CFC-12) hydrodechlorination (6, 7) motivated us to test the direct redox method developed by Barbier *et al.* (15, 26). Prior to the discussion on Pd–Au characterization, a comment concerning the preparation method seems appropriate. The direct redox method makes profit from the fact that noble metal ions are reduced by zerovalent species of less noble metals; as such a redox reaction is driven by the difference in standard electrochemical potential. In our case, i.e., deposition of gold on palladium in a chloride solution led to a certain dissolution of palladium, most probably due to the reaction: $Pd + 4Cl^- \leftrightarrow PdCl_4^{2-} + 2e^-$. In addition, some gold also remained in solution. Nevertheless, the resulting silica-supported solids, after chemical analysis was performed, constituted suitable precursors for preparation of well-mixed Pd–Au catalysts.

A combination of X-ray diffraction, temperature-programmed palladium hydride decomposition, and catalytic probing (hydrogen chemisorption and 2,2-dimethylpropane conversion) allowed us to characterize the state of Pd–Au bimetal in SiO_2-supported catalysts at various stages of their preparation. Analysis of the results obtained conclusively indicates a substantial degree of Pd–Au mixing. Therefore, the direct redox method can be recommended for preparation of Pd–Au/silica catalysts.

3.1. X-ray Diffraction Study of Pd–Au/SiO_2

X-ray diffraction appeared very useful in assessing variations in the structure and phase composition of Pd–Au/SiO_2 samples at various stages of preparation. Figure 3 illustrates variations for the $Pd_{0.80}Au_{0.20}$(A) sample prepared from 1.1 wt% Pd/SiO_2. It is demonstrated that upon deposition practically two fractions of highly dispersed material coexist: almost pure palladium and gold phases (upper profile).

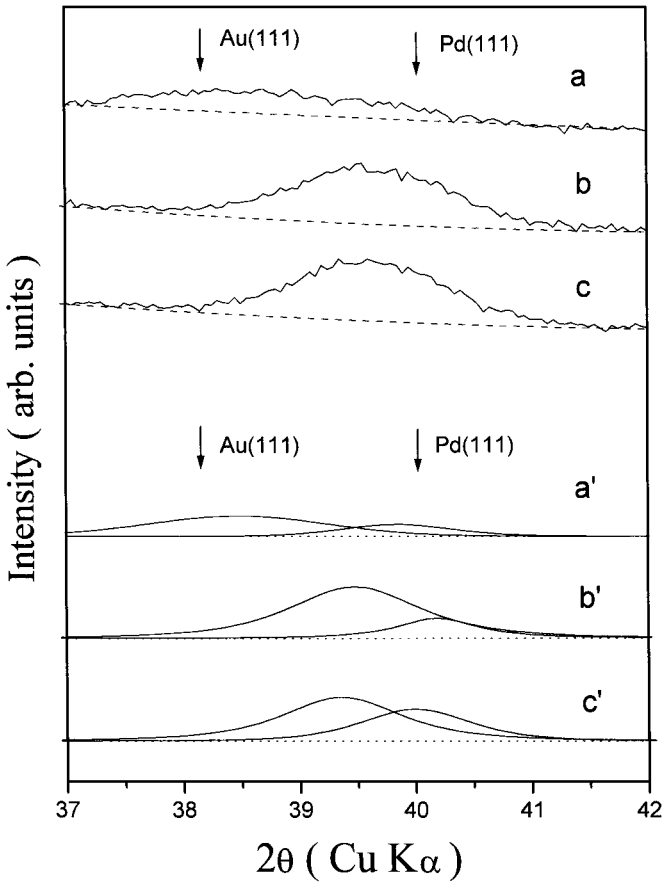

FIG. 3. XRD profiles of $Pd_{0.80}Au_{0.20}$ catalyst prepared from 1.1 wt% Pd/SiO_2. (a, a′) As prepared; (b, b′) after 1-h reduction; (c, c′) after 3-h reduction. Top section, experimental data; bottom section, profile decomposition into Pearson VII-type functions.

Although some presence of Pd–Au alloy(s) in the precursor should not be ruled out, nevertheless, at this point of discussion it is reasonable to assume that if the detected phases are in direct contact, the gold-rich phase must cover the Pd-rich phase. Such a conclusion follows from the preparation method. The reduction in flowing H_2/Ar at 400°C brings about a marked transformation (middle and bottom profiles): the gold-rich material has disappeared and only the phase with Pd–Au composition comparable to the nominal bimetal composition is found in addition to a small amount of nearly pure Pd phase. Therefore, it is logical to assume that a considerable degree of Pd–Au mixing resulted from the preparation method; i.e., gold was placed onto palladium particles or in their very close vicinity. In the opposite case, as in our previous work (10) when palladium and gold had been deposited by coimpregnation (using the silica support and chloride solutions), even a prolonged reduction in flowing hydrogen would not result in proper alloy homogeneity (10).

Duration of reduction (1 or 3 h) at 400°C does not seem to have a pronounced effect on the XRD patterns (Fig. 3). This probably follows from the fact that 1-h reduction at 400°C is sufficient for intermixing two very thin layers of Pd and Au. Incidentally, O Cinneide and Clarke (27) prepared homogeneous Pd–Au films by evaporation and subsequent annealing in hydrogen at 450°C for 1 h. Since the thickness of their films was in the range 50–100 nm and Pd–Au particles in the present work are much smaller (~10 nm), the extensive intermixing obtained by us after 1-h reduction is understandable. The presence of a residual amount of nearly pure palladium after reduction (Fig. 3) indicates that some, albeit small, part of palladium has not been covered with gold after its deposition. Table 2 summarizes XRD data obtained for all bimetallic catalysts (series A and B). It is evident that considerable Pd–Au alloying occurs.

Decomposition of a complex (111) diffraction peak into a few component reflections indicates the presence of bimetallic particles of 10–15 nm in size (Fig. 3). This may correspond to metal dispersion of the order of 0.1, which is in agreement with hydrogen chemisorption data for $Pd_{0.90}Au_{0.10}$(A) and $Pd_{0.80}Au_{0.20}$(A) catalysts (D_h, Fig. 8). The fact that mean crystallite sizes (from XRD profile broadening) are in fair agreement with respective data calculated from chemisorption experiments suggests that our XRD profile decomposition was justified.

TABLE 2

Phase Composition of Pd–Au/SiO_2 Catalysts after Reduction at 400°C (Series A and B)

Catalyst[a]	Reduction time (h)	Metal phase composition detected by XRD
		Series A
$Pd_{0.90}Au_{0.10}$	1	Almost pure Pd phase + ~15 at.% Au
	3	Almost pure Pd phase + ~25 at.% Au
$Pd_{0.80}Au_{0.20}$	1	Almost pure Pd phase + larger amounts of ~32 at.% Au[b]
	3	Almost pure Pd phase + ~37 at.% Au[b]
		Series B
$Pd_{0.95}Au_{0.05}$	1	Large size Pd crystallite fraction overlapping a dispersed 5 at.% Au phase
	3	As after 1 h
$Pd_{0.80}Au_{0.20}$	1	Large crystallites of almost pure Pd (~8 at.% Au) + ~60 at.% Au + ~37 at.% Au[c]
	3	Large crystallites of almost pure Pd (~1.5 at.% Au) + a more diffused phase of ~25 at.% Au[c]
$Pd_{0.60}Au_{0.40}$	1	Large crystallites of almost pure Pd + two more diffused phases of ~45 and ~55 at.% Au
	3	Small amount of large crystallites of almost pure Pd + two more diffused phases of ~25 and ~50 at.% Au

[a] as in Table 1.
[b] XRD profile shown in Fig. 3.
[c] XRD profile shown in Fig. 4.

XRD spectra of Pd–Au samples prepared from 2 wt% Pd/SiO_2 (series B) are more complex. It is recalled that the precursor material has already been inhomogeneous, i.e., composed of some big metal crystallites coexisting with an almost amorphous palladium (see Experimental). It should also be mentioned that so great an extent of heterogeneity created low reproducibility of XRD spectra. This problem imposed XRD scanning of several samples of the same material and selection of the most representative spectra. The presence of a sharp, intensive diffraction peak from the Pd-rich phase (Fig. 4) overlapping diffuse reflection(s) from highly dispersed phase(s) renders our interpretation less unambiguous than that in the case of samples prepared from 1.1 wt% Pd/SiO_2. The basis for profile decomposition was an assumption that the fitted peak widths for all phases (apart from the additional sharp peak belonging to poorly dispersed palladium) should be comparable. Thus, the $Pd_{0.80}Au_{0.20}$(B) sample from 2 wt% Pd/SiO_2 showed the presence of both Pd-very rich and Au-rich phases, in addition to non-negligible amounts of mixed Pd–Au fcc phases, characterized by values of lattice parameters of 0.3938 nm (25 at.% Au) and 0.3983 nm (48 at.% Au). One-hour reduction of this precursor leads to marked changes (Fig. 4, middle profile): both highly dispersed Pd-rich and Au-rich phases disappear, giving rise to Pd–Au alloy phases. However, the sharp peak attributed to big Pd crystallites is essentially unaltered. Three-hour hydrogen treatment vastly diminishes the intensity of the latter reflection (bottom profile), suggesting that a prolonged reduction at 400°C effects a considerable Pd–Au mixing, even in the case of massive palladium particles.

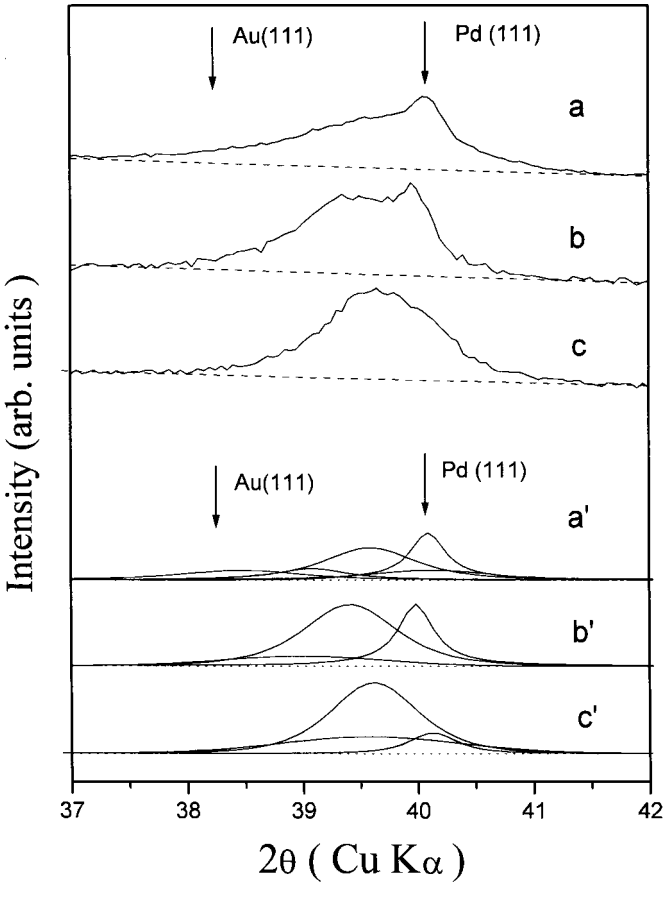

FIG. 4. XRD profiles of $Pd_{0.80}Au_{0.20}$ catalyst prepared from 2 wt% Pd/SiO_2. (a, a′) As prepared; (b, b′) after 1-h reduction; (c, c′) after 3-h reduction. Top section, experimental data; bottom section, profile decomposition into Pearson VII-type functions.

Summing up, the XRD results (Figs. 3 and 4, Table 2) show that reduction of Pd–Au catalyst precursors prepared by a direct redox method leads to considerable alloying of both metals. Homogenization lasts longer when dealing with bigger metal crystallites (catalysts of series B, prepared from 2 wt% Pd/SiO_2). However, in the case of a highly dispersed Au/Pd sandwich layer (catalysts of series A, obtained from 1.1 wt% Pd/SiO_2), such an intermixing is faster and needs only 1 h. This must be an effect of close proximity of Au and Pd guaranteed by the method of Au deposition onto Pd/SiO_2. The possibility that during reduction at 400°C a considerable portion of metal would effectively migrate over the support to form bimetallic particles is less realistic. In our previous attempt in preparing silica-supported Pd–Au catalysts the incipient wetness coimpregnation from chloride solution resulted in highly dispersed metal catalysts (10). However, even a prolonged reduction (15 h at 380°C) could not produce a reasonable alloying of both metals.

3.2. Temperature-Programmed (Palladium) Hydride Decomposition (TPHD)

Our present knowledge about the formation and decomposition of the β-PdH phase formed from supported palladium catalysts (25, 28–32) suggests that the position, shape (width, distortion), and intensity of a TPHD peak should depend on different variables, among which Pd dispersion, type of support, and modifying additives play a dominant role. Therefore, to probe the effect of Pd alloy composition in supported catalysts, the other variables should be separated. It has been demonstrated (31) that the isotherms of hydrogen absorption–desorption in/from supported Pd/β-PdH show hysteresis loops that have more poorly defined plateau pressure compared to that of the unsupported Pd black and hysteresis continuing beyond the normally accepted two-phase regions. For our discussion of the temperature-programmed β-PdH decomposition, it is important to notice that the course of decomposition of the β-phase depends on a support, even when the catalysts are poorly dispersed and not too highly reduced (e.g., at 200°C, Ref. (31)). The effect of support should be removed or greatly reduced, when one uses the same carrier for all the catalysts tested. In addition, to avoid metal–support interactions, high reduction temperatures should not be applied.

In conclusion, before probing of Pd–Au/SiO_2 bimetallic catalysts is considered, we discuss the results obtained for monometallic Pd/SiO_2 catalysts having different metal dispersions. The effect of Pd particle size on the stability of the β-PdH phase and especially on the H/Pd ratio (25, 32) imposes such investigation.

3.2.1. Monometallic Pd/SiO_2 catalysts. TPHD trace of highly dispersed 1.1 wt% Pd/SiO_2 catalyst (FE = 0.55, d_{Pd} = 2 nm, 1.12/FE, (33)) shows only a small amount of hydrogen liberated at temperature below 100°C (H/Pd = 0.03, Fig. 5). Gradual application of more drastic pretreatment conditions leads to the decrease of metal dispersion (FE) and amplifies the negative peak in the TPHD trace (Fig. 5). Finally, reduction of a wet catalyst resulting in a severe metal sintering (FE ~ 0.05) amplifies this peak markedly and the H/Pd ratio approaches the value close to that considered for bulk β-PdH (0.6, (28)).

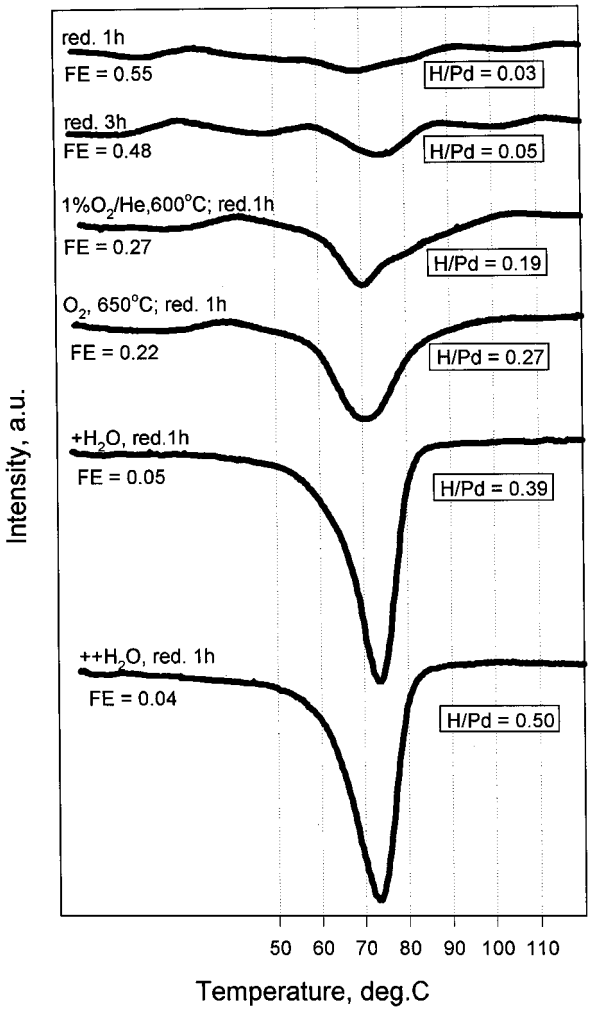

FIG. 5. Temperature-programmed hydride decomposition (TPHD) profiles of differently pretreated 1.1 wt% Pd/SiO_2 (series A). Catalyst pretreatments, metal dispersions (FE), and the H/Pd ratios are marked at the respective TPHD profile.

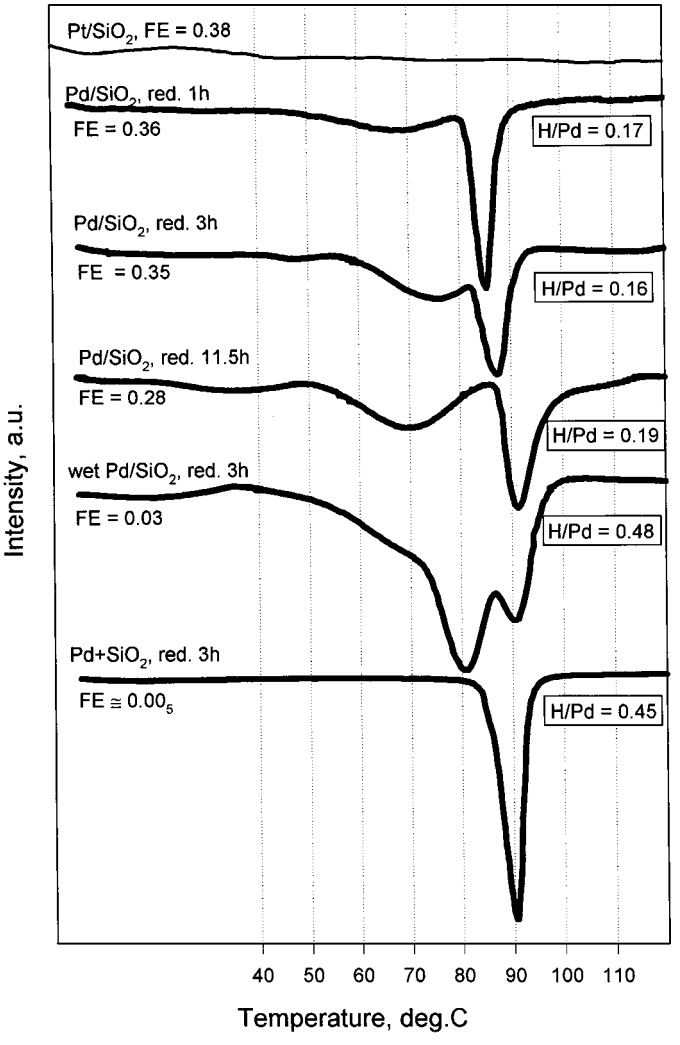

FIG. 6. TPHD profiles of differently pretreated 2 wt% Pd/SiO_2 (series B). Catalyst pretreatments, metal dispersions (FE), and the H/Pd ratios are marked at the respective TPHD profile.

On the other hand, the position of the minimum in TPHD traces does not seem to depend distinctly on metal dispersion. Such a result seems to be surprising, as one suspects lower stability of a hydride phase in highly dispersed Pd catalysts. Different observations were reported earlier in this respect. A correlation between the d_{Pd}, H/Pd ratio, and position of the minimum in the TPHD spectrum is noticed in the study by Pinna *et al.* on silica-supported Pd catalysts (34). The same group, however, observes TPHD spectra of various palladium catalysts centered at ~80°C (18). Therefore, one is rather far from a universal correlation ($T_{min} = f(FE)$); other variables are probably also important.

Figure 6 shows the results for 2 wt% Pd/SiO_2, Pd(B) catalyst. Insertion of a featureless profile obtained for Pt/SiO_2 emphasizes the exceptional behavior of palladium catalysts in such experiments (platinum does not form bulky hydride phases). It is recalled that Pd(B) was characterized by bi-

modal distribution of metal particles (XRD, Fig. 1). Very big crystallites (∼100 nm in size) coexisted with finely dispersed palladium (∼3 nm). Now, the TPHD spectra look different than those presented for Pd(A), (Fig. 5). A very intense minimum is centered at ∼90°C. In addition, a rather diffused negative peak at ∼70°C develops after applying more drastic reduction conditions. Confrontation of the TPHD trace of Pd(A) with the complementary result with a physical mixture of Pd powder and silica allows us to ascribe the "90°C" peak to hydrogen evolution from a massive palladium hydride. On the other hand, the low-temperature peak ("70°C") must be associated with a more finely dispersed Pd, comparable to Pd(A). As judged from the H/Pd ratio (assuming H/Pd of 0.6 for a crystalline PdH), the fraction of a less-dispersed material is ∼15% and does not seem to increase during gradual sintering of the starting sample.

Considering the results obtained for both Pd/SiO_2 catalysts, it is concluded that the H/Pd ratio correlates well with palladium dispersion, like the previous data reported by others (25, 32) (see Fig. 7). Somewhat lower H/Pd ratios obtained in this work are probably due to the fact that the cited works (25, 32) furnished equilibrium solubility data, collected at isothermal conditions. On the other hand, the temperature of the minimum in the TPHD spectrum is not a simple function of metal dispersion (FE). It does not depend much on FE for the range 0.04–0.55, i.e., for a Pd particle size between ∼2 and ∼30 nm. The apparent shift in decomposition temperature, from ∼70 to ∼90°C, is realized only when palladium sinters to very big Pd crystallites.

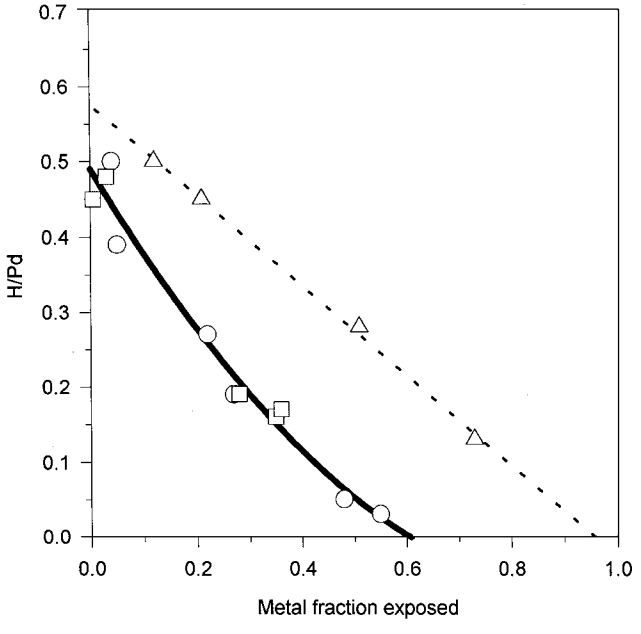

FIG. 7. H/Pd ratios obtained in TPHD experiments with silica-supported catalysts. Circles represent data for differently pretreated Pd(A) and squares for Pd(B) samples. Triangles represent hydrogen solubility (in Pd/SiO_2) data estimated from Fig. 6 in Ref. (25).

Such a picture is supported by the results of Newbatt *et al.* (31), where very different shapes of hysteresis (Pd ⇄ PdH) loops in the case of various palladium catalysts are shown. The course of PdH decomposition from a Pd black sample indicated a clear-cut decomposition process (Fig. 1a in Ref. (31)). In the isothermal experiment, hydrogen pressure over the sample had to be drastically decreased to a very low value at which the hydride could be decomposed. In contrast, a mildly dispersed Pd/SiO_2 (FE = 0.05) formed a hydride phase, which was decomposing in a "sluggish" process; i.e., decomposition started at relatively high hydrogen pressure and continued for a considerable pressure range (Fig. 1b in Ref. (31)). We assume that such a specimen-specific course of PdH decomposition under isothermal conditions can be transposed onto the course of TPHD, i.e., decomposition of the hydride phase from Pd black needs a higher temperature than the analogous process associated with Pd/SiO_2.

3.2.2. Bimetallic Pd–Au/SiO_2 catalysts. The chemisorption data show a marked decrease in hydrogen consumption when Pd/SiO_2 catalysts are doped with gold. This decrease may result from a reduced, compared to pure Pd, chemisorption capability of Pd–Au clusters. Another reason is due to an overall decrease of metal dispersion. Since the deposition of gold onto palladium takes place in an aqueous solution, the precursor after the redox reaction is wet. During preparation of Pt–Au/SiO_2 catalysts by a redox reaction, Barbier *et al.* (26) also found a marked decrease in the overall metal dispersion.

Temperature-programmed experiments concern the Pd–Au catalysts at various stages of their preparation. An absence of a hydrogen consumption peak in TPR profiles indicates that reduction is finished at the beginning of the experiment (i.e., due to flowing H_2/Ar at ∼0°C), (Fig. 8). Instead, one observes a negative β-hydride decomposition peak, which is shifted toward higher temperatures by 10–15°C, compared to the TPHD profile of 1.1 wt% Pd/SiO_2(A) (Fig. 5). Since the XRD study showed the presence of two phases (Pd-rich and Au-rich, Fig. 3), it is clear that the presence of an Au-rich phase must influence the decomposition of a hydride phase formed in the Pd-rich phase. In the discussion of XRD spectra of the Pd–Au catalysts, it has been accepted that a majority of the Au-rich phase covers the Pd-rich phase. This leads to the conclusion that the presence of a thin layer of gold (or gold-very rich alloy) on top of palladium particles results in some delay in hydrogen release to the gas phase. The subsequent TPHD run performed on the same catalysts prereduced at 400°C for 1 h shows that the hydride decomposition peak is shifted backward to the position characteristic for pure palladium. Extension of reduction time from 1 to 3 h does not make any changes in TPHD spectra for the bimetallic samples. This result, in coincidence with XRD data, indicates that in the case of Pd–Au bimetallic samples prepared from

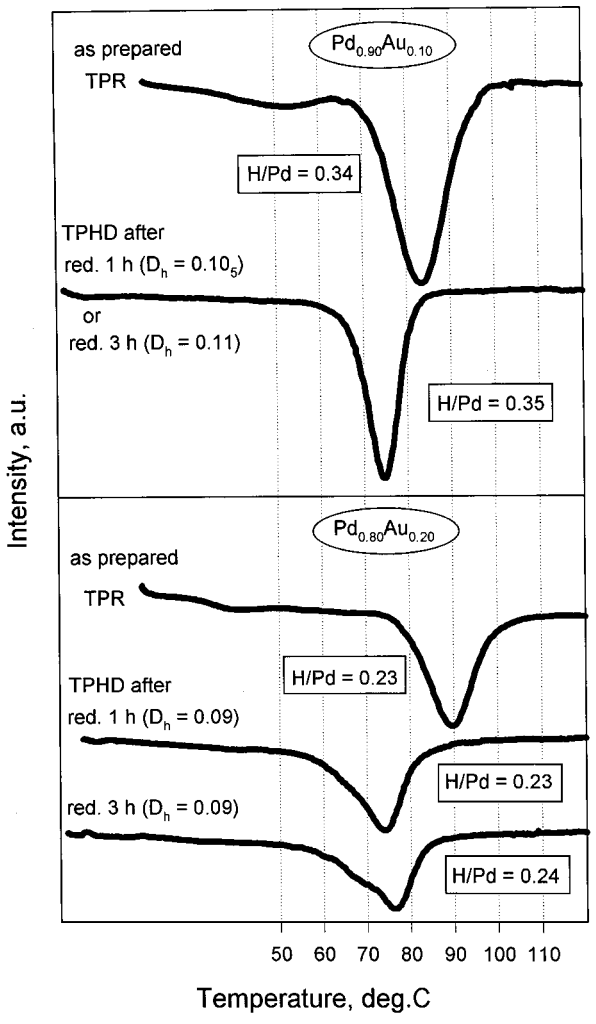

FIG. 8. Temperature-programmed experiments on Pd–Au catalysts prepared from 1.1 wt% Pd/SiO_2 (series A). Top profiles are TPR traces; remaining profiles are from TPHD experiments.

1.1 wt% Pd/SiO_2, the reduction period of 1 h is sufficient to form stable, bimetallic particles.

The situation with the bimetallics prepared from 2 wt% Pd/SiO_2 is somewhat complicated by the fact that the starting catalyst had bimodal distribution of metal particles of a finely dispersed material coexisting with big palladium crystallites. Deposition of gold onto such an inhomogeneous material results in a situation where the presence of a small particle fraction is not manifested by TPHD spectra (Fig. 9). After 1-h (and 3-h) reduction of $Pd_{0.95}Au_{0.05}$(B), the H/Pd ratio from hydride decomposition is close to 0.5, i.e., the value characteristic for pure Pd (Fig. 6). It seems that the finely dispersed Pd-based material essentially disappeared after gold deposition. In addition, the course of TPHD run resembles the one obtained during the experiment with wet 2 wt% Pd/SiO_2 (Fig. 9): two intense minima at relatively high temperatures are observed (termed as "70°C" and "90°C" in the preceding subsection, see also Fig. 6). As discussed earlier, the minimum at ~90°C in the TPHD profile of 2 wt% Pd/SiO_2 is attributed to the hydride decomposition from very big Pd crystallites. Since metal dispersion (FE) of such a material is <0.05, the addition of only 5 at.% Au should completely cover Pd particles, if Au is predominantly deposited on palladium. Figure 9 shows that TPHD profiles are not dependent on reduction time (1 vs 3 h).

TPHD spectra obtained for the two other Au-richer samples are similar to those shown by $Pd_{0.95}Au_{0.05}$(B) (Fig. 9, middle and bottom parts). The only difference is that now the presence of the coarse Pd-based material is better manifested. This is especially well seen for $Pd_{0.60}Au_{0.40}$(B). The satellite peak at 70°C, attributed to a more dispersed palladium that is very intense for $Pd_{0.95}Au_{0.05}$(B), gradually disappears with gold addition, whereas the "90°C" peak is almost unchanged. This suggests that a majority of introduced gold is alloyed with palladium, constituting a more dispersed phase, whereas big Pd crystallites are not modified. For $Pd_{0.60}Au_{0.40}$(B) only the high-temperature peak

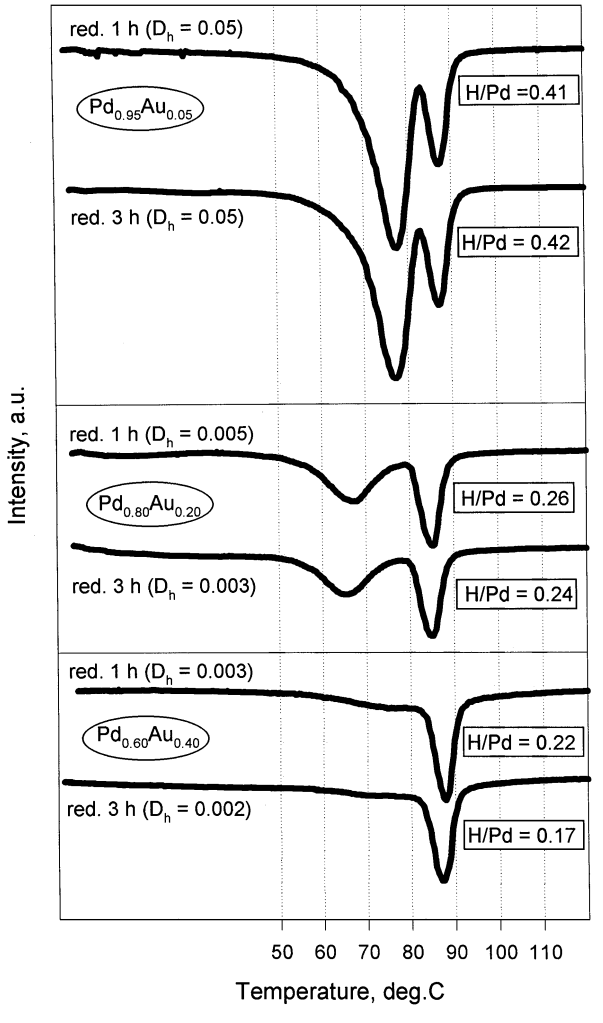

FIG. 9. TPHD profiles (after 1- and 3-h reduction) from Pd–Au catalysts prepared from 2 wt% Pd/SiO_2 (series B).

TABLE 3

2,2-Dimethylpropane Reaction on Pd–Au/SiO_2 Catalysts Prepared from 1.1 wt% Pd/SiO_2 (Series A): Turnover Frequencies, Selectivities, and Activation Energies

Catalyst	Reduction duration, h	Reaction temperature, °C	α^a, %	TOF[b], 1/s	Selectivity, %[c] $S_{C<5}$	Selectivity, %[c] S_{is}	E_A, kJ/mol
$Pd_{0.90}Au_{0.10}$[d]	1	240	0.07	1.35×10^{-4}	68.5	31.5	
		250	0.20	3.99×10^{-4}	67	33	256 ± 4
		260	0.66	1.31×10^{-3}	73	27	
	3	240	0.08	1.40×10^{-4}	70	30	
		250	0.25	4.65×10^{-4}	69	31	258 ± 3
		261	0.79	1.44×10^{-3}	76	24	
$Pd_{0.80}Au_{0.20}$[d]	1	251	0.13	1.99×10^{-4}	75.5	24.5	
		260	0.31	4.56×10^{-4}	75	25	222 ± 7
		270	0.87	1.29×10^{-3}	80	20	
	3	260	0.20	3.14×10^{-4}	69.5	30.5	
		270	0.47	7.26×10^{-4}	72	28	197 ± 4
		275	0.70	1.05×10^{-3}	76	24	

[a] Conversion in %.
[b] Based on dispersion data displayed in Fig. 8.
[c] Product selectivity: $S_{C<5}$, to hydrogenolysis products; S_{is}, to iso- and *n*-pentane.
[d] For catalyst code, see text.

is seen and the H/Pd ratio from hydride decomposition amounts to 0.17 (after 3-h reduction). The low value of the H/Pd ratio observed for a low dispersed Pd-based catalyst confirms that a considerable part of Au is dissolved in Pd crystallites.

3.3. Catalytic Probing of Pd–Au/SiO_2 Catalysts

Previous results (10) showed only small changes in the catalytic behavior of 2 wt% Pd–Au/SiO_2 catalysts prepared by incipient wetness coimpregnation. Turnover frequency, product selectivity, and activation energy in 2,2-dimethylpropane conversion exhibited only insignificant changes with nominal bimetal composition (10). Those data indicated an absence of significant Pd–Au interaction. For instance, the apparent activation energy was practically unchanged in the range 0–50 at.% Au (~210 kJ/mol). In comparison, for two commercial Pd–Au powders, the apparent activation energy was markedly lower than the respective value for palladium powder. Estimated values from data in Table 4 in Ref. (10) are $E_A(Pd) > 300$ kJ/mol, $E_A(Pd_{0.25}Au_{0.75}) \sim 200$ kJ/mol, and $E_A(Pd_{0.20}Au_{0.80}) \sim 190$ kJ/mol. Analogous estimation of kinetic data for Pd–Au films (35) provides results that are coincident with the supposition that the addition of gold to palladium should decrease the activation energy in 2,2-dimethylpropane conversion. In addition, another work with monometallic Pd/SiO_2 catalysts (36) showed that for low and moderate Pd dispersions (FE between 0 and 0.3, i.e., comparable with the present catalysts) apparent activation energy was higher than 250 kJ/mol and not very sensitive to metal dispersion. Therefore, any marked decrease in activation energy obtained as an effect of Au doping would be ascribed to Pd–Au alloying and not to variations in metal dispersion. Our results (Tables 3 and 4) show that, indeed, a progressive doping of Pd catalysts with Au gradually decreases the activation energy. Two Pd-rich samples from each series ($Pd_{0.90}Au_{0.10}$, Table 3, and $Pd_{0.95}Au_{0.05}$, Table 4) show relatively high values of E_A. On the other hand, the remaining samples, with higher Au content, exhibit much lower E_A. Therefore, their behavior, comparable to that exhibited by Pd and Pd–Au powders (10), speaks again for a considerable Pd–Au alloying obtained in our Pd–Au/SiO_2 catalysts.

Such a conclusion is compatible with literature data on other metal catalysts. Modification of Ru/SiO_2 by adding IB metal leads to different situations, depending on whether Cu or Ag is added (37). More extensive Ru–Cu interaction results in significant changes in activation energy in ethane hydrogenolysis from 167 kJ/mol, for Ru/SiO_2, to 130 kJ/mol, for $Ru_{0.60}Cu_{0.40}$ (Table 2 in Ref. (37)). In contrast, an analogous doping with silver caused only marginal changes in E_A. This finding, supported by other results (XRD, chemisorption, XPS), suggested the presence of Ag islands (not atomically dispersed) on a ruthenium surface (37).

Analysis of our selectivity data (Tables 3 and 4) is less conclusive. Previous expectations on the enhancement of the isomerization selectivity (at the expense of hydrogenolysis) with Au introduction to Pd (10) is not confirmed by the present results. Only small selectivity variations have been observed (Tables 3 and 4). It should, however, be noticed that, in the case of 22DMP conversion on Pd-containing catalysts, the isomerization selectivity depends very much on the extent of overall conversion since isopentane

TABLE 4

2,2-Dimethylpropane Reaction on Nondoped and Au-Doped 2 wt% Pd/SiO_2 (Series B): Turnover Frequencies, Selectivities, and Activation Energies

Catalyst	Reduction duration, h	Reaction temperature, °C	α^a, %	TOF[b], 1/s	Selectivity, %[c] $S_{C<5}$	Selectivity, %[c] S_{is}	E_A, kJ/mol
Pd[e]	3	271	0.14	5.73×10^{-4}	61	39	
		276	0.26	1.05×10^{-4}	61	39	324 ± 5
		283	0.67	2.69×10^{-3}	65	35	
$Pd_{0.95}Au_{0.05}$[d]	1	256	0.19	9.16×10^{-4}	71	29	
		263	0.44	2.10×10^{-3}	70.5	29.5	279 ± 1
		270	0.99	4.69×10^{-3}	74	26	
	3	260	0.17	3.20×10^{-4}	64	36	
		270	0.54	1.01×10^{-3}	65	35	280 ± 2
		280	1.63	3.05×10^{-3}	73	27	
$Pd_{0.80}Au_{0.20}$[d]	1	285	0.23	6.90×10^{-3}	76	24	
		293	0.39	1.14×10^{-2}	74	26	153 ± 5
		300	0.57	5.02×10^{-2}	72.5	27.5	
	3	270	0.18	4.28×10^{-3}	70.5	29.5	
		280	0.36	8.70×10^{-3}	67	33	173 ± 6
		290	0.62	1.49×10^{-2}	64	36	
$Pd_{0.60}Au_{0.40}$[d]	1	303	0.10	2.58×10^{-3}	58	42	
		313	0.19	4.93×10^{-3}	58	42	181 ± 4
		323	0.35	8.90×10^{-3}	59	41	
	3	300	0.05	2.25×10^{-3}	51.5	48.5	
		310	0.09	4.50×10^{-3}	51	49	165 ± 3
		320	0.16	7.98×10^{-3}	51.5	48.5	

[a, c, d] As in Table 3.
[b] Based on dispersion data, see Figs. 6 and 9.
[e] Wet 2 wt% Pd/SiO_2, Pd(B), reduced at 400°C for 3 h.

(primary product) is much more reactive than the reactant thus it is readily converted into hydrogenolysis products. It should also be added that in their study with Pt–Au/SiO_2 catalysts Foger and Anderson (38) found that the isomerization selectivity increased initially with increasing gold content reaching a maximum and then started to decrease. More recently, Balakrishnan and Schwank (39) did not notice any special changes in the isomerization selectivity upon adding gold to Pt/SiO_2. Although both groups suggested various interpretations of their results, one has to come to the general conclusion that the isomerization selectivity cannot constitute a convenient diagnostic parameter toward determining whether or not gold is well mixed with palladium or platinum in supported catalysts.

4. CONCLUSIONS

Two series of Pd–Au/SiO_2 catalysts, with differently dispersed metal phase particles, were prepared by a direct redox method. The method, developed by Barbier *et al.* (15, 26), appeared very useful because significant Pd–Au alloying was accomplished in all silica-supported bimetallic catalysts. The catalysts were probed by X-ray diffraction and temperature-programmed hydride decomposition at various stages of their preparation. These techniques were found valuable in assessing the degree of alloying. Being sensitive to palladium particle size, the temperature-programmed hydride decomposition (TPHD) would also be used in estimation of palladium dispersion.

2,2-Dimethylpropane conversion carried out on Pd–Au/SiO_2 also appeared to be a useful probe. Apparent activation energy decreased considerably with gold addition. This was not the case for Pd–Au/SiO_2 catalysts prepared by an incipient wetness coimpregnation (our earlier work (10)) when the resulting bimetallic samples were not satisfactorily homogenized.

REFERENCES

1. Rylander, P. N., "Catalytic Hydrogenation over Platinum Metals." Academic Press, New York, 1967; Rylander, P. N., "Catalytic Hydrogenation in Organic Synthesis." Academic Press, London, 1979.
2. Arnold, H., Döbert, F., and Gaube, J., *in* "Handbook of Heterogeneous Catalysis" (G. Ertl, H. Knözinger, and J. Weitkamp, Eds.), Vol. 5, Chap. 4.4, p. 2165. Wiley VCH, Weinheim, 1997.
3. Abel, R., Collins, P., Eichler, K., Nicolau, I., and Peters, D., *in* "Handbook of Heterogeneous Catalysis" (G. Ertl, H. Knözinger, and J. Weitkamp, Eds.), Vol. 5, Chap. 4.6.5.4B, p. 2298. Wiley VCH, Weinheim, 1997.

4. Rao, V. N. M., U.S. Patent 5 447 896 (1995), to du Pont de Nemours.
5. Morikawa, S., Samejima, S., Yositake, M., and Tatsematsu, S., European Patent 0 347 830 A2 (1989), to Asahi Glass Co.
6. Malinowski, A., Juszczyk, W., Pielaszek, J., Bonarowska, M., Wojciechowska, M., and Karpiński, Z., *Chem. Commun.* 685 (1999).
7. Malinowski, A., Juszczyk, W., Pielaszek, J., Bonarowska, M., Wojciechowska, M., and Karpiński, Z., *in* "Proceedings, 12th International Congress on Catalysis, Granada, 2000" (A. Corma, F. V. Melo, S. Mendiovos, and J. L. G. Fierro, Eds.), Elsevier, Amsterdam, 2000.
8. Bond, G. C., *Chem. Soc. Rev.* **20**, 441 (1991).
9. Allison, E. G., and Bond, G. C., *Catal. Rev.* **7**, 233 (1973).
10. Juszczyk, W., Karpiński, Z., Łomot, D., Pielaszek, J., and Sobczak, J. W., *J. Catal.* **151**, 67 (1995).
11. Inami, S. H., and Wise, H., *J. Catal.* **26**, 92 (1972).
12. Sancier, K. M., and Inami, S. H., *J. Catal.* **11**, 135 (1968).
13. Lam, Y. L., and Boudart, M., *J. Catal.* **50**, 530 (1977).
14. Davis, R. J., and Boudart, M., *J. Phys. Chem.* **98**, 5471 (1994).
15. Barbier, J., *in* "Handbook of Heterogeneous Catalysis" (G. Ertl, H. Knözinger, and J. Weitkamp, Eds.), Vol. 1, Chap. 2.2.1.6., p. 257. Wiley VCH, Weinheim, 1997.
16. Chang, T.-C., Chen, J.-J., and Yeh, C.-T., *J. Catal.* **96**, 51 (1985).
17. Lieske, H., Lietz, G., Hanke, W., and Völter, J., *Z. Anorg. Allg. Chem.* **527**, 135 (1985).
18. Benedetti, A., Fagherazzi, G., Pinna, F., Rampazzo, G., Selva, M., and Strukul, G., *Catal. Lett.* **10**, 215 (1991).
19. Xu, L., Lei, G.-D., Sachtler, W. M. H., Cortright, R. D., and Dumesic, J. A., *J. Phys. Chem.* **97**, 11517 (1993).
20. Ohnishi, R., Wang, W.-L., and Ichikawa, M., *Appl. Catal. A* **113**, 29 (1994).
21. Malinowski, A., Juszczyk, W., Bonarowska, M., Pielaszek, J., and Karpiński, Z., *J. Catal.* **177**, 153 (1998).
22. Łomot, D., *Pol. J. Chem.* **72**, 2598 (1998).
23. Maeland, A., and Flanagan, T. B., *J. Phys. Chem.* **69**, 3575 (1965).
24. Joice, B. J., Rooney, J. J., Wells, P. B., and Wilson, G. R., *Discuss. Faraday Soc.* **41**, 223 (1966).
25. Boudart, M., and Hwang, H. S., *J. Catal.* **39**, 44 (1975).
26. Barbier, J., Marécot, P., Del Angel, G., Bosch, P., Boitiaux, J. P., Didillon, B., Dominguez, J. M., Schifter, I., and Espinoza, G., *Appl. Catal. A* **116**, 179 (1994).
27. O Cinneide, A., and Clarke, J. K. A., *J. Catal.* **26**, 233 (1972).
28. Scholten, J. J. S., and Konvalinka, J. A., *J. Catal.* **5**, 1 (1966).
29. Palczewska, W., *Adv. Catal.* **24**, 245 (1975).
30. Lewis, F. A., "The Palladium/Hydrogen System." Academic Press, New York, 1967.
31. Newbatt, P. H., Sermon, P. A., and Luengo, M. A. M., *Z. Phys. Chem. N.F.* **147**, 105 (1986).
32. Bonivardi, A. L., and Baltanás, M. A., *J. Catal.* **138**, 500 (1992).
33. Ichikawa, S., Poppa, H., and Boudart, M., *J. Catal.* **91**, 1 (1985).
34. Pinna, F., Signoretto, M., Strukul, G., Polizzi, S., and Pernicone, N., *React. Kinet. Catal. Lett.* **60**, 9 (1997).
35. Karpiński, Z., *J. Catal.* **77**, 118 (1982).
36. Karpiński, Z., Butt, J. B., and Sachtler, W. M. H., *J. Catal.* **119**, 521 (1989).
37. Rouco, A. J., Haller, G. L., Oliver, J. A., and Kemball, C., *J. Catal.* **84**, 297 (1983).
38. Foger, K., and Anderson, J. R., *J. Catal.* **61**, 140 (1980).
39. Balakrishnan, K., and Schwank, J., *J. Catal.* **132**, 451 (1991).